Joint Centre for Mesoscale Meteorology, Reading, UK

Cold Pools in Shear

D. J. Parker

Internal Report No. 51

September 1995

Met Office Joint Centre for Mesoscale Meteorology Department of Meteorology
University of Reading PO Box 243 Reading RG6 6BB United Kingdom
Tel: +44 (0)118 931 8425 Fax: +44 (0)118 931 8791
www.metoffice.com

Designed and produced by the Met Office © Crown copyright 2001 01/0240 The Met Office logo is a registered trademark.

COLD POOLS IN SHEAR

Douglas J. Parker

Department of Meteorology,
University of Reading.

Abstract

Gravity currents exist in many forms and develop within many types of flow. The dynamics of long-lived cumulonimbus are thought to be strongly influenced by the interaction of a spreading pool of cold low level air, which may act as a gravity current, and the ambient sheared flow in the boundary layer. In interpreting two and three dimensional numerical models of such phenomena, the balance of vorticity between the ambient flow and the spreading cold air is commonly invoked. In order to investigate these vorticity balance ideas from a gravity current perspective, three dimensional numerical simulations have been performed in which a cold pool spreads from an isolated source in the presence of a horizontal flow which is sheared with height. It has been found that the shear of the incoming ambient flow does not qualitatively alter the behaviour of the spreading cold pool, nor does it alter the location of the region of maximum horizontal convergence: the actual strength of the ambient wind has a greater bearing on the cold pool shape than the shear. Consequently, it must be the details of the moist convection which play a crucial role in determining the cold pool's development in sheared flows. As such, this model is a general indication of the robustness of gravity current theory, even in the presence of mean shear. The vortex structure on the flanks of the spreading cold air is found to be significantly modified, with a reversal in the dominant sign of vorticity and an increase in its intensity, when such mean shear exists.

1. Introduction

Gravity currents (also known as density currents) are phenomena which occur universally in the field of fluid mechanics, as the flow of anomalously buoyant fluid against a horizontal or inclined surface. The wide range of examples of these phenomena includes avalanches and mudslides, oil spillages on the sea and dense gas releases (Simpson, 1982). In meteorology, intense convective storms generate regions of intense precipitation: the cold air at low levels which is produced by evaporative cooling of the falling precipitation is believed to behave locally as a gravity current. In particular, it is the convergence and forced lifting at the front of the low level cold air mass (or cold pool) which is believed to be responsible for the triggering of further moist convection and the consequent long-lived behaviour of systems such as 'supercells' or 'squall lines'. The nature of the cold pool front—its depth and intensity of convergence—determines its potential for triggering new cells.

Crucial to the dynamics of such long-lived storm systems is the ambient wind profile, in particular the shear of the low level wind with height. In quasi-two dimensional systems such as squall lines, this shear is seen to interact with the two dimensional cold pool and allow the convection to be continually coupled to the cold head to give a positive reinforcement: the cold head triggers convection; the resulting precipitation evaporates and feeds the low level cold air. It is argued that unless a suitable low level shear exists in the ambient flow, the convection and cold pool will not favourably interact (Thorpe, Miller and Moncrieff, 1982; Rotunno, Klemp and Weisman, 1988). Furthermore, it has been shown how favourable shear, directed away from the cold air, gives a deeper cold pool head and greater lifting of potentially buoyant moist air (Xu, 1992).

From a three dimensional perspective there are further consequences of the interaction between the cold pool and the ambient shear and it is the behaviour of a three dimensional gravity current from a local source, in the presence of an ambient shear with height, that is considered here. Authors such as Weisman (1993) show how, at a storm-generated cold pool in the presence of shear, tilting of horizontal vortex tubes over the cold head, coupled with stretching by the relatively high vertical velocities associated with the moist convection, can lead to coherent horizontal 'bookend' vortices (vertical component of vorticity) on the flanks of the cold pool, of roughly circular form. Tilting down of the vortex tubes by an intense

convective downdraught may induce vortices of the opposite sign, corresponding to a 'rear-inflow' jet above the head of the cold pool. As in the two dimensional case, the wind above the cold pool head determines its depth and the likelihood of triggering of convection, so the position, sign and intensity of the mesoscale vortices helps determine the location at which further convection will occur. A feedback may result, as the subsequent convection provides the cooled downdraughts which supply the cold pool, and their position may affect the shape of the cold pool, and hence the storm, as it develops. In addition, the wind over the cold air will modify the speed of the cold pool front, and hence have a direct influence on its shape. In cases where there was some delay between the genesis of new storm cells, this direct influence may predominate.

Despite the common occurrence of mesoscale vortex development in numerical storm simulations, it is not clear to what extent the vortex deformation and the stretching are controlled by the existence of the moist convection in the atmosphere above the cold air. In the bow echo simulations of Weisman (1993), tilting by the evaporatively forced downdraughts of the bow echo is required to produce the dominant vortices, which have the opposite sign to those which would be produced simply by tilting at the edge of the cold pool. Recent cloud-model studies of Davis and Weisman (1994) have indicated that the dominant vorticity source is in the elevated mesoscale circulation of a mature system. It remains to be seen whether the formation of vortices above the cold pool head is a 'gravity current' phenomenon or whether it is a coherent aspect of deep, long-lived convective storms, independent of the low level cold air. Other studies, such as those of Droegemeier and Wilhelmson (1985a,b) which show the shape of the cold pool to be influenced by the ambient shear strength, likewise include moist convection.

In many parts of the world, the winds and precipitation associated with organised storms can be extremely destructive: other well known effects of the vorticity generation at active cumulomimbus systems include the formation of tornadoes. Forecasting these phenomena is clearly of great importance.

Synoptic fronts which form within larger scale atmospheric development often exhibit intense moist convection and it has been suggested that on the mesoscale the dynamics may be similar to those of squall lines, with the front behaving locally like a gravity current which triggers

further convection. Certainly, squall lines are often observed to be initiated by the convection at a synoptic front (Meischner *et al.*, 1991). Since the synoptic front is formed as the intensification of large scale temperature gradients while the cold pool is generated locally by evaporative cooling, the behaviour of a cold pool in non-trivial large-scale flow must be appreciated if the propagation and stability of convective synoptic fronts is to be understood. The behaviour of isolated cold pools in shear flow may have a bearing on the behaviour of localised anomalies to a cold front.

It is the purpose of the present work simply to model a spreading region of cold air in an ambient shear, using numerical simulations, to assess whether the vortex structure and winds which develop as the cold pool spreads are able to modify the cold pool behaviour in the absence of convection. This work is directed principally at the meteorological context of storm-generated cold pools. Such systems have height scales of order 1 km and cover horizontal distances of $100's$ of km over a period of hours: as such, a relatively limited parameter regime is explored here. However, the conceptual simplicity of the problem means that the results may apply in more general arenas.

2. Gravity currents

The essential theory of high Reynolds number gravity currents such as these (review by Simpson, 1982) expresses the front speed, U_f, as being determined by a Froude number balance, with,

$$U_f = k\sqrt{g'h}, \tag{1}$$

where g' is the buoyancy difference, h a height of the gravity current and k is a constant, effectively the Froude number and generally found to be of order unity (dependent on the fractional depth of the gravity current). When an ambient flow is present, laboratory (two dimensional) and observational studies find a linear relationship between the front speed and the ambient wind speed, of the form,

$$U_f = k\sqrt{g'h} - bU_0, \tag{2}$$

with U_0 the oncoming flow. A positive value of U_0 means ambient flow directed towards the cold air locally and will tend to retard the front's progress (reduce U_f). This relation appears to hold for both positive and negative values of U_0 and Simpson and Britter (1980) give values of $k = 0.9$ and $b = 0.6$; Thorpe *et al.* (1980), from two dimensonal numerical studies, found $k = 1.0$ and $b = 0.7$.

When a gravity current flows from a local source in three dimensions, it will tend to become shallower and propagate more slowly with increasing radius from the source because of the requirement of constant mass-flux with radius in a steady flow. A volume integral over an upright cylinder centred on and enclosing the source expresses this analytically: using the divergence theorem,

$$B \equiv \int_V \frac{gQ}{\theta_0} d^3\mathbf{r} = 2\pi r_c \int g'u dz, \tag{3}$$

where V is the volume of the cylinder and u the radial velocity, assuming laminar flow through the cylinder boundary and steady flow in which $\frac{\partial g'}{\partial t} = 0$ within the cylinder. For a uniform gravity current of constant density anomaly and speed with depth, this gives a closure between the speed and the buoyancy flux, B, of,

$$B = 2\pi r g' h u, \tag{4}$$

for any r behind the gravity current head. If it is then taken that the front speed of the gravity current is a constant fraction, α, of the speed of the following flow, as indicated by Simpson and Britter (1980), (4) may be evaluated just behind the head to give,

$$B = 2\pi r_f g' h(\alpha U_f) = \frac{2\pi\alpha r_f}{k^2}(U_f)^3, \tag{5}$$

in which (1) has been used. This is a relationship between the speed of the front, $U_f = \frac{dr_f}{dt}$, and its distance, r_f, from the source, so it may be integrated to give the distance of advance with time. When B is taken to be a constant (as in the case of constant cooling), the solution is,

$$r_f = \left(\frac{4}{3}\right)^{\frac{3}{4}} \left(\frac{k^2 B}{2\pi\alpha}\right)^{\frac{1}{4}} (t - t_0)^{\frac{3}{4}} \tag{6}$$

This functional relationship is in agreement with a scaling solution of Britter (1979) which was a good fit to the results of laboratory experiments (B is equivalent to Britter's $Q_1 g'$).

As a consequence of (6),

$$U_f \sim B^{\frac{1}{4}} (t - t_0)^{-\frac{1}{4}}, \tag{7}$$

and,

$$U_f \sim B^{\frac{1}{3}} r_f^{-\frac{1}{3}}, \tag{8}$$

so the front speed decreases monotonically with time and distance from the source; the depth of the flow similarly decreases, through (1).

If an ambient flow were imposed on this system, invoking the formula (2) at the leading edge of the current would suggest that the front may become stationary when,

$$U_f|_0 = bU_0, \tag{9}$$

where $U_f|_0 = k\sqrt{g'h}$ is the speed of the current in the absence of ambient flow, a decreasing function of time. However, in such a situation the gravity current will not be axisymmetric, in depth or velocity, and the analysis outlined above will not be valid. In particular, the upstream edge of the cold pool will be deeper and will tend to have an increased speed against

the environmental flow. Subsequently it will be shown how the stagnation of the leading edge occurs. (9) should be seen as providing time and distance scales (through (7) and (8)) for the retardation of such a gravity current by larger-scale flow.

In stratified atmospheric flows, (1) is often approximated, invoking the hydrostatic balance, to be,

$$U_f = k_1 \sqrt{\frac{\Delta p}{\rho_r}}, \tag{10}$$

in which Δp is the surface pressure drop as the front passes, ρ_r is a reference density and k_1 is constant, again generally found to be order unity. For the analysis of the results obtained using this numerical model, (10) has been used, since it may be computed accurately and relates more directly to pressure perturbations observed as such mesofronts pass ground sites. As remarked by Smith and Reeder (1988), the evaluation of Δp is not, in the general atmospheric case, unambiguously determined. For instance, if the pressure is not uniform behind the head of the current, as in the axisymmetric laboratory experiments of Britter (1979) where it rises towards the dense source, it is not clear how to evaluate Δp. One option, which has been followed here, is to use the pressure difference between the ambient air at the surface and that below the raised head of the current. A constant value of ρ_r is used—the surface air density of $\rho_r = 1.23\ kgm^{-3}$.

In the initial state of these numerical simulations, an extremely low static stability is used, corresponding to a Brunt-Väisälä frequency of $N = 10^{-4} s^{-1}$, in order to maintain the simplicity of the problem. As a consequence, the overall Froude number of the flows, defined as $Fr \equiv \frac{U_f}{Nh}$, is always large: Simpson (1982) describes how gravity currents at lower Froude numbers may exhibit more complex behaviour, such as the interaction with a train of gravity waves and the formation of multiple fronts. This behaviour was also discussed in the context of numerical simulations by Raymond and Rotunno (1989). While the use of a small value of static stability precludes such gravity wave interactions, it does mean that when shear is present, the imposed ambient flow exhibits an extremely low value of the Richardson number, $Ri \equiv \left(\frac{N}{\frac{dU_0}{dz}}\right)^2$, suggesting that Kelvin-Helmholtz instability may occur. However, the basic states used in these simulations do not exhibit such instability.

3. The Numerical Model

Accurate numerical modelling of gravity currents requires sophisticated turbulence closure, a realistic lower boundary condition and fine resolution. However, since the principal objective of this study is to simulate the bulk influence of the negatively buoyant flow on the vorticity dynamics, and the feedback with the developing flow, it is not thought that such sophistication is necessary, provided the limitations of a simple model are not evaded. Just as the 2-level model of Benjamin (1968) remains an important conceptual tool in the understanding of the dynamics of fully turbulent gravity currents, it is hoped that the three dimensional numerical model will illuminate a more general problem. Hence, a relatively simple diffusion scheme is included in the simulations and a free-slip boundary condition is used. Diffusion is necessary since, as shown by Benjamin (1968), a steady gravity current solution in a deep fluid requires energy loss near the head of the current. In practice, without diffusion the gravity current depth is shallow and determined by the vertical resolution. The diffusion scheme used here is Richardson number dependent and described by Miranda (1990).

The model used is the nonhydrostatic sigma-coordinate model of Miranda (1990), with a resolution of $2.5km$ in the horizontal and equally-spaced sigma levels (typically 20; validated with 40), giving higher vertical resolution nearer the ground. Boundary conditions are a rigid surface and a lid at 500 mb (roughly 5 km), with radiative lateral boundaries, designed to minimise gravity wave reflections (Miranda, 1990).

The horizontal resolution is chosen to be sufficiently fine that the square grid does not give an asymmetry to the spreading air and the results are insensitive to the horizontal resolution used here: the response of the cold air to an inflow is independent of the direction of the inflow on the square grid. In particular, to produce circular symmetry in the absence of ambient flow, the source region must be sufficiently well resolved; generally, the spreading gravity current will tend to preserve its initial shape for long periods when in a quiescent environment. The results are insensitive to the vertical resolution provided diffusion is used, as described above, and the cold air is sufficiently deep that it is spanned by a sufficient number of model levels: in practice at least 5 levels are required to give any consistency in the representation of the flow and this should be borne in mind when studying cloud model results.

Cold gravity currents are initiated by constructing a cylindrical cooling region between

fixed sigma levels (the depth of the cooling is approximately 3.75 km, as may be seen from the column of cold air in figure 6). The cooling is constant in time with a profile of the form of a cosine with horizontal radius and constant with height, having width 15km and variable maximum amplitude, Q. The specification of Q can be used to provide cold pools of differing intensities. Typically $Q = -120\ Khr^{-1}$, which is relatively large compared with that of Thorpe *et al.* (1980) who took $Q \sim -30\ Khr^{-1}$. The cooling region is fixed in the domain and in the general simulations, there is flow relative to this region aloft. This may be thought to contradict observations that cloud systems tend to propagate with a velocity close to that of the winds above the boundary layer. However, the source used here remains an artificial one, constructed solely to provide gravity currents of the correct characteristics close to the ground.

Inevitably, when studying numerical results such as these, the available parameter space can not be explored exhaustively. In this paper, the more qualitative results are illustrated with reference to several cases of selected ambient wind profiles which seem to be typical of certain types of behaviour, as in figure 1. The wind profiles are determined by two parameters, the ground-level wind and the (constant) shear up to a height of 3 km, both oriented in the x-direction. The results are organised into the discussion of four regimes; those of (a) zero ambient flow, (b) uniform ambient flow with no shear, (c) ambient flow with moderate shear up to 3 km and (d) very intense ambient shear. To maintain the simplicity of the system, planetary rotation is ignored.

4. Results

(a) Gravity current simulation

In order to test the qualitative validity of the simulated gravity currents, axisymmetric cold sources of differing intensities have been used in a quiescent environment. In each simulation, the varying front speed of the spreading current gives a large number of values of U_f and $\sqrt{\frac{\Delta p}{\rho_r}}$. Various authors have made theoretical, experimental and numerical calculations of the values of k_1 and b (in (2) and (10)) for two dimensional gravity currents (Smith and Reeder, 1988): it is not the purpose of this study to make an accurate assessment of these parameters, especially since it would be possible to use far more sophisticated numerical codes to perform the simulations. However, it was found that after an initial adjustment period of the order of 1 hour, the flows reached a balance between front speed and pressure gradient equivalent to $k_1 \sim 1.2$, confirming that the numerical solutions do indeed represent gravity current behaviour. More significantly, the solutions agree with the functional form of (6), verified by Britter's (1979) laboratory experiments. For instance, with a source of 120 Khr^{-1}, the solution exhibits a form $r_f \sim t^{\kappa}$, with $\kappa = 0.73$. In this case, over a period of two hours, the front speed falls from around 18 ms^{-1} to around 10 ms^{-1} while the frontal pressure rise is of the order of 1 mb, also decreasing with time: these values are comparable with observed atmospheric cases.

(b) Uniform ambient flow

Linden and Simpson (1994) describe laboratory experiments on point source gravity currents in a cross-flow and in is of interest to compare their results with the numerical model used here. Simple simulations of the circular source in the presence of uniform ambient flow indicate that the front remains approximately circular as it spreads: in an ambient flow of 10 ms^{-1} the axes of the cold pool from a source of 120 Khr^{-1} differ by around 3% (figure 1(b)). The front spreads in a frame which moves at a speed which is proportional to the ambient flow. This result may be expressed in the form,

$$U_c = \beta U_0, \tag{11}$$

where U_c is the speed of the centre of the cold air (calculated as the centre of the axis aligned along the wind direction) and β is a constant, found to be approximately $\beta = 0.65$ in these

simulations, for a range of wind of $5\ ms^{-1} < U_0 < 15\ ms^{-1}$. Note that it is not strictly correct to equate β with b in (2) since the variation of height between the upstream and downstream edges of the current means that $\sqrt{\frac{\Delta p}{\rho_r}}$ will be larger at the upstream edge and lower at the downstream edge, implying a relative 'propagation' upstream. However, since computed values of b and β seem to be numerically close to one another, it may be reasonable to approximate $\beta = b$.

When the ambient flow becomes sufficiently strong to produce stagnation at the leading edge, significant change in the shape occurs. This is illustrated in figure 1(c), in which the source of $120\ Khr^{-1}$ lies in an environmental flow of $-20\ ms^{-1}$. In this figure, the bold contour is plotted at $3000\ s$, the time at which the speed of this current in a quiescent environment, $U_f|_0$, would fall to $0.65U_0$, satisfying (9). From figure 1(c) it appears that this is approximately the point at which the nose becomes stationary, and the point beyond which the shape of the current differs markedly from circular: more accurate calculation of the nose speed with time shows that the front has become almost stationary at a time of around $3,500\ s$. Beyond this time, the leading edge of the gravity current does not retreat, despite the fact that $U_f|_0$ falls below $0.65U_0$. This is because the depth of the cold air remains high. There is cold air continually generated at the source and the front must remain upstream of this region: the source determines the frame of reference by which stagnation may be seen to happen. Thus it appears that (9) is a useful estimate for the time beyond which cold pool characteristics change in a uniform flow.

The head of the cold pool remains upstream of the source after stagnation has been reached. This implies a change in the nature of the gravity current, in that the source is fixing the upstream buoyancy flux and maintaining the depth with time, so that the cold air can remain steady in the opposing flow. Klemp *et al.* (1994) note how two dimensional gravity currents propagating against a uniform flow move faster than predicted by Benjamin's (1968) formula, and ascribe this to the fixed buoyancy flux supplied by the source: predicting the behaviour of the gravity current then requires knowledge of the source conditions. In the three dimensional case discussed here, there is also evidence of this effect in the cases with weaker ambient flow, in that the upstream nose of the cold air seems to have propagated faster than other parts of the front, causing a mild departure from circular shape.

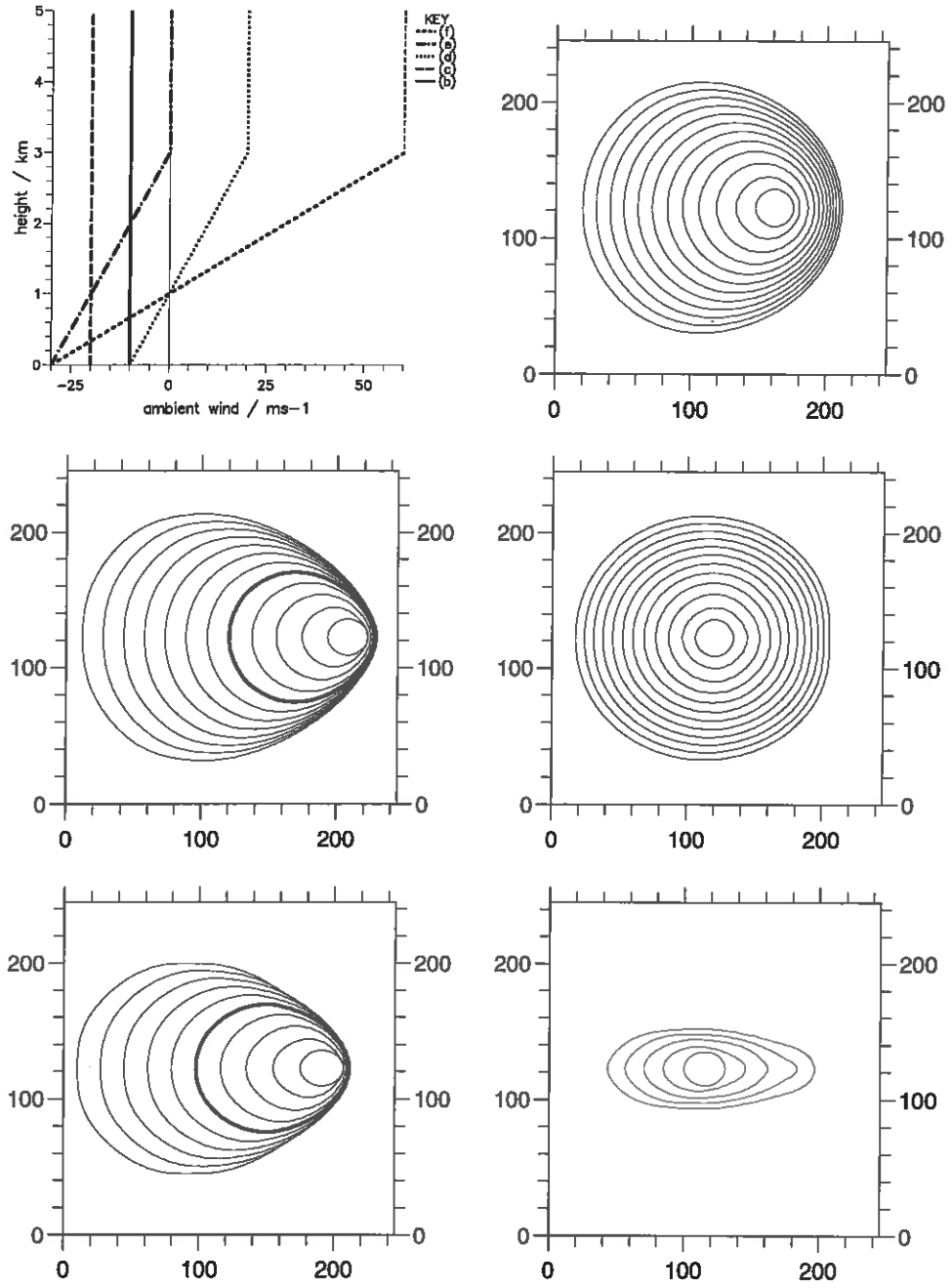

Figure 1: Successive positions of the $\theta' = -1K$ contour on the lowest model level, with time, as an indication of the developing shape of the cold pool front as it spreads, for the principal cases described in the text. (a) Ambient wind profiles with height for each case; (b) $U_0 = -10ms^{-1}$ (solid line profile in (a)); (c) $U_0 = -20ms^{-1}$ (long dashes); (d) $U_0 = -10ms^{-1} + 10ms^{-1}km^{-1} \times z$ (dotted); (e) $U_0 = -30ms^{-1} + 10ms^{-1}km^{-1} \times z$ (dot-dashed); (f) $U_0 = -30ms^{-1} + 30ms^{-1}km^{-1} \times z$ (short dashes). Axes in km: contours are plotted every 10 minutes; the bolder contour is at 50 minutes.

Linden and Simpson's (1994) work indicates that the upstream front is shallower than the downstream front, in apparent contradiction with the results shown here, and elsewhere, for storm-generated cold pools. Linden and Simpson's (1994) experiments were performed with an elevated source in which the descending fluid, initially driven by its momentum, rapidly adjusts through entrainment to become a buoyant plume and it is likely that the upstream buoyancy flux in their experiments was not required to be as large as that in numerical cases where the turbulent entrainment is not parametrized. In these numerical examples the rapidly descending cold air seems to move horizontally along the ground away from the source region as a momentum jet, adjusting through mixing to become a buoyancy-driven flow. Recall that in the absence of ambient flow, there was an initial adjustment period during which the cold pool speed exceeded the densimetric speed, suggesting jet-like behaviour. This remains a potential inconsistency in the discussion of how an ambient flow influences a cold pool head, and returns to the issue of the influence of the source on 'free' gravity current behaviour. Such topics would be interesting areas for further work.

If, in the numerical simulations, the source of cold air is switched off after $2,700s$, the free gravity current adjusts so that upstream and downstream fronts have the same depth. Since there is a free slip lower boundary condition, such a gravity current may propagate as an near-axisymmetric flow in a frame moving with the ambient wind. Thus, the lower boundary condition may also be important in determining cold pool depth.

Since the front is deeper in the direction facing the oncoming wind, it is at this point that deeper lifting of the oncoming air occurs, regardless of whether the front reaches a stagnation point. In the context of convective storms, triggering of new cells would be expected to be favoured at this leading edge of the cold pool, when no shear is present. However, it must be appreciated that although deeper lifting will favour condensation and cell generation at that point, the flow above the cold pool is also crucial to determining whether coherent cells may occur.

(c) Vertically-sheared ambient flow: moderate shear

Inclusion of shear in the flow ambient to a three dimensional gravity current from a local source is a problem that would be difficult to simulate experimentally. However, it is relatively simple to modify the basic state flow of the numerical model used here and to make a direct

comparison with the results for more simple formulations.

Two principal results of this study are that the shape of a spreading cold pool, as viewed from above, is not markedly changed by the presence of ambient vertical shear and that, bound up with this, coherent circular vortices are not seen to form above the cold air. The vertical vorticity generated by tilting of the ambient horizontal vortex tubes is confined to thin strips on the flanks of the cold pool. As a corollary, the singular shape and mesoscale vorticity structure of the cold pools of modelled convective storms appears to be controlled by an interaction with the moist convection, rather than an interaction with the ambient flow.

Figures 1(d), 2(b) and 2(d) show results for a case in which $Q = -120\ Khr^{-1}$ and the ambient shear profile has strength $\frac{d\overline{u}}{dz} = 10ms^{-1}km^{-1}$ over the lowest $3km$—a relatively strong shear for atmospheric flows, but not an unphysical one. The ground level wind here is $\overline{u} = -10ms^{-1}$. It can be seen from the plot of successive positions of the front (figure 1(d)) that the spreading cold pool experiences only a slight change in plan-view shape, when compared with the marked deforming of a cold pool seen in figure 1(c), despite the strong ambient shear and the difference in front height between upstream and downstream edges (figure 2(b)). Straightening of the downshear front is evident in figure 1(d), and this is not an interaction with the boundary or grid orientation as it is invariant to changing wind orientation. However, it does not represent a dramatic change in the curvature of the front, considering the timescales involved here: these simulations have been integrated for over 3 hours and extend for hundreds of km as compared with storm cell lifetimes of the order of 20 minutes and scales of order $10km$. The plot of vertical velocity (figure 2(b)) confirms this impression: the maximum of upward flow forced by the baroclinicity at the head is at the leading edge of the cold pool.

Comparison between the cases with and without ambient shear (figure 2) shows that the effect of the shear is to increase the asymmetry between forced upward motion at the upstream and downstream edges of the cold pool. There is an indication that the shear produces a deeper and more intense updraught, as suggested by Rotunno *et al.* (1988), at the cold pool leading edge, though it is difficult to quantify this effect here, since the cold pools have different intensities of temperature perturbation.

The steering level for the centre of this gravity current (calculated as the mid-point of the along-wind axis) is at around 850 m, of the order of the height of the current. If the wind is

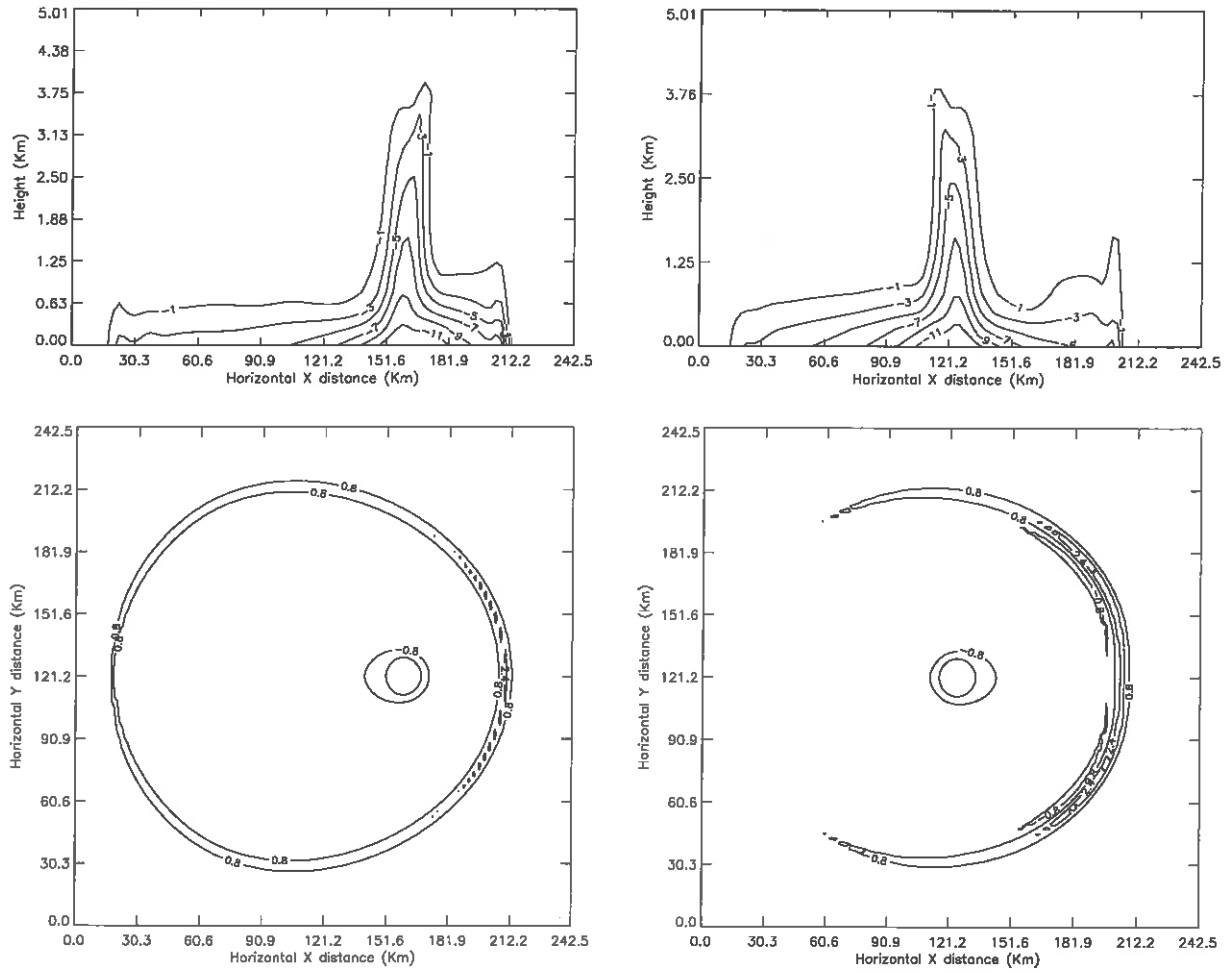

Figure 2: Plots of θ and w for the case illustrated in figures 1(b) (uniform ambient flow) and 1(d) (sheared ambient flow), respectively: (a) and (b) vertical sections of potential temperature through the cold air on an axis along the direction of ambient shear (contours labelled in K); (c) and (d) the field of vertical velocity in a horizontal plane at height $750m$, in which the most intense forced upward motion is in an arc stretching around the leading edge of the cold pool (contour interval 1.6 ms^{-1}).

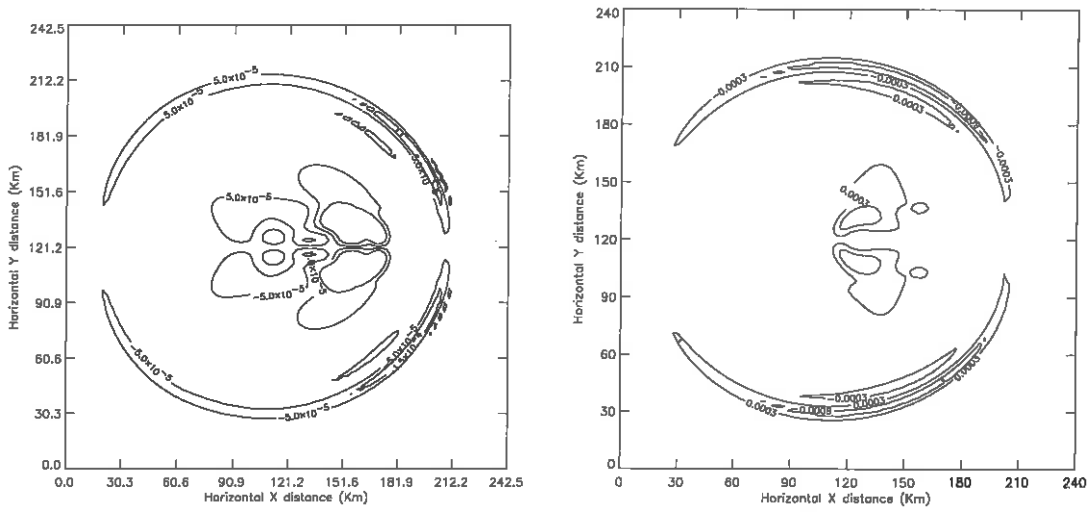

Figure 3: The vertical component of vorticity in a horizontal plane at height $750m$, for the (a) uniform 10 ms^{-1} and (b) 10 $ms^{-1}km^{-1}$ sheared inflows (both have the same wind at ground level). In the absence of shear, the vorticity is most intense in strips to the flanks of the cold air, positive to the north and negative to the south. When shear is included vertical vorticity of the opposite sign and greater magnitude is produced, outside the cold air. Contour intervals are (a) $10^{-4}s^{-1}$ and (b) $6 \times 10^{-4}s^{-1}$.

reduced by 20 ms^{-1} at all levels (so the shear is unchanged but the surface wind is $-30ms^{-1}$), the leading edge reaches stagnation (figure 1(e)) and a form similar to that discussed in the previous section (and figure 1(c)) develops, with a considerable departure from circular shape. It seems that the magnitude of the wind influences the shape of the cold pool more strongly than the shear, when stagnation occurs at the leading edge.

Vorticity dynamics: zero shear

The vorticity dynamics of this flow may be seen in terms of traditional ideas of 'tilting' of horizontal vortex tubes. In the absence of ambient flow, the baroclinicity at the front and near the cold source generates horizontal vorticity within the cold pool, from the solenoidal term in the vorticity equation. The vortex tubes are closed circles parallel to the front and with no vertical component. Without tilting of these vortex tubes there is no vertical component of vorticity.

When an ambient wind is imposed, as in the $U_0 = -10$ ms^{-1} case discussed above, this gives an asymmetry to the previously axisymmetric problem. The flow is no longer purely in

the radial/vertical plane and the source region itself produces a complicated pattern of vertical vorticity (figure 3(a)), although away from the source and the front this vorticity is weak, less than $5 \times 10^{-5} s^{-1}$. At the front, the cold pool becomes deeper in the upwind direction and has greater upward motion in this region, providing a mechanism for tilting of the horizontal vorticity generated baroclinically in the gravity current, by differential lifting of vortex tubes parallel to the front. Also, any component of vorticity *normal* to the front, generated by *horizontal* tilting of the horizontal vorticity in the cold air, will be tilted vertically as it meets the updraught at the front.

Along the symmetry axis of the cold pool, parallel to the ambient wind, where the gravity current vortex tubes remain parallel to the front, an understanding of the vorticity sources due to along-front tilting can be acheived. Figure 4(a) shows a cross section along this axis, through the leading edge of the cold pool. Within the cold pool the horizontal y-component of vorticity, η, reaches less than $-2 \times 10^{-2} s^{-1}$. At the front itself, however, this vorticity reduces smoothly to a value of zero in the irrotational ambient flow. The front is actually a transition zone of finite thickness, as may be seen in the gradients of η and θ, and it is across this transition zone that the upward motion occurs. Since the upward motion is stronger at the leading edge than at other locations around the cold pool front, along-front tilting of the y-vorticity, η, generates vertical vorticity of magnitude $1.5 \times 10^{-4} s^{-1}$ on the flanks of the cold pool, positive to the north and negative to the south. This vorticity is confined to narrow strips on the flanks of the cold pool. On the inner side of these strips there is vertical vorticity of the opposite sign; this represents the same sign as that of the background vertical vorticity of the cold pool on each side of the symmetry axis, generated in the source region. However, these locally intense strips are not likely to be due to 'stretching' of the cold pool vorticity since they occur in a region of downward motion. Rather, they may be seen as the tilting down of negative y-vorticity as the vortex tubes at the leading edge bend back down behind the raised nose of the gravity current. This may be inferred from figure 4(a) in which downward velocity may be seen behind the front, where η is negative.

Vorticity dynamics: sheared ambient flow

The above situation shows how vertical vorticity may be produced at a cold pool by the imposition of an ambient wind, without the presence of environmental shear. When shear is

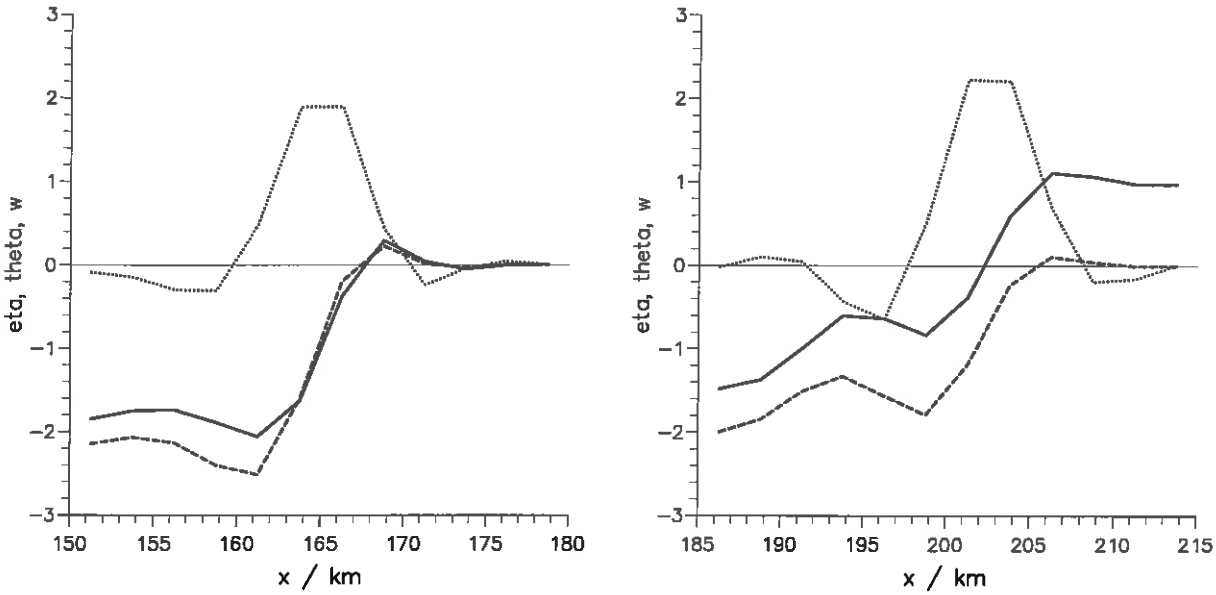

Figure 4: The potential temperature (dashed, /K), vertical velocity (dotted, $/ms^{-1}$) and y-vorticity, η (solid, $/10^{-2}s^{-1}$) on a cross-section through the cold pool front, at the position of maximum x-extent, for **(a)** uniform ambient wind $-10ms^{-1}$ and **(b)** ambient shear of $10ms^{-1}km^{-1}$.

introduced into the ambient flow, here $10ms^{-1}km^{-1}$, an added degree of complication arises. In the vicinity of the source region, significant vertical vortices occur, as in figure 3(b). These vortices correspond to a local maximum in u, along the wind-axis of the gravity current. This phenomenon is an illustration of the way in which tilting down of horizontal ambient vorticity in a region of diabatic cooling can produce a 'rear-inflow' jet, as described by Weisman (1993). This does not occur in the absence of environmental shear. However, here this is not related to the cold pool dynamics but simply to the behaviour of the cooling region. The existence of this rear-inflow does not seem to have a strong influence on the spreading cold pool. With a direct convective feedback in a cloud model, a rear inflow over the head might encourage triggering of further convection in that region.

As in the unsheared case, the generation terms at the source and within the gravity current yield relatively low values of vertical vorticity behind the head (apart from in the source region), but of the opposite sign to those which occur in the absence of shear. Away from the source region, the significant pattern of vertical vorticity structure occurs at the cold front. As before, the analysis of the vortex dymanics at the head of the current is somewhat more straightforward

on the flow, or shear, axis, in the downshear direction. In this case, figure 4(b) shows how the finite thickness frontal zone at which the upward motion occurs represents a transition between the negative y-vorticity of the gravity current ($\eta < -2 \times 10^{-2} s^{-1}$ further behind the front) and the positive y-vorticity of the environmental flow ($\eta = 10^{-2} s^{-1}$). Consequently, along-front tilting is able to produce vertical vorticity of both signs on each flank of the gravity current. Figure 3(b) shows how the tilting of the positive environmental y-vorticity in the frontal zone has produced a strip of vertical vorticity outside that which occurs in the absence of environmental shear, and of the opposite sign. This is a significant result, in that the presence of vertical shear in the ambient flow reverses the sign of the vorticity observed on the flanks of the cold pool. However, the vertical component of vorticity, although attaining large values (over $10^{-3}\ s^{-1}$), is not organised into the coherent vortices seen in convective storm simulations. Again, the vorticity appears at the edge of the cold pool in narrow strips at each flank.

Although the ambient y-vorticity is a factor of 2 smaller than that within the gravity current, the vertical vortices to the flanks of the cold pool are an order of magnitude more intense than those which occur without ambient shear. In order to explain this difference, it is helpful to consider the component of horizontal vorticity *normal* to the front. Away from the front, the ambient vortex tubes are aligned in the y direction and on the flanks of the gravity current this is a normal component of vorticity. Figure 6 confirms that the normal component of vorticity (shear in the x direction) remains significant close to the flank of the gravity current. Tilting of this normal component (i.e. cross-front tilting) occurs as a vortex tube lies across the narrow updraught zone: this mechanism is more efficient than differential lifting of vortex tubes aligned tangentially to the updraught zone. Figures 5 and 6 show that the normal vorticity, η, outside the flank of the gravity current in the shear flow, is stronger and of an opposite sign to that within the gravity current. The gravity current horizontal vorticity remains principally tangential to the front whereas on the flanks, the external vorticity has a strong normal component and can generate much more intense vertical vorticity through tilting. These observations explain why the vortices in the case with ambient shear are displaced downstream from the leading edge of the cold pool.

Figure 3(b) indicates that a vorticity strip again occurs within the principal one, of opposite sign. At this altitude ($750m$), the inner vortex strip lies within the cold air and should be

attributed to the generation mechanisms discussed previously, for the unsheared basic state (that is, tilting *up* of cold pool *negative* vorticity), rather than to tilting down of ambient vorticity over the cold pool nose. By inference from figure 4(b), a third, innermost strip of vorticity may be expected to occur, attributable to the tilting *down* of *negative* cold pool y-vorticity. Although the third, inner strip is not seen explicitly in these results, it is consistent with an observed reduction in the background vertical vorticity of the gravity current. In all, the combination of the two principal strips of vorticity of opposite sign implies an elevated maximum of upshear horizontal flow, or elevated jet, on each flank of the cold pool, coinciding with the temperature front (figure 6). The jets are absent in the absence of shear in the ambient flow (figure 5). Their strength is appreciable: such flanking jets may have a bearing on storm development but it should be recalled that different vortex structure tends to be seen when convective latent heating occurs above the cold pool. In storm simulations with meso-vortices above the cold pool, jets occur above the cold front, and can modify the behaviour of a storm.

Although in these simulations no instability of the flanking vortex strips is seen, such instability would be a potential source of vortex roll-up and locally intensified convergence. It is possible that the convergence at the cold pool front suppresses growth of instabilities: this topic would be an interesting area of further study.

Since the production of vertical vorticity depends on the tilting of the negative horizontal vorticity of the cold pool and the positive horizontal vorticity of the ambient flow, the structure of the finite width frontal zone must be well represented. For more accurate resolution of the dynamics of this region, an appreciation of the intimate dynamics of mixing would be needed, including surface drag and 'overrunning' by the cold air: such detail is not attempted here.

The values of relative vorticity obtained here are high compared with large scale atmospheric values; the typical planetary vorticity, $f \sim 10^{-4}\ s^{-1}$ in the midlatitudes. The origin of the environmental wind shear, or horizontal component of vorticity, is frictional processes in the boundary layer: tilting of the horizontal vortex tubes produces regions of strong positive and negative vertical vorticity. Any stretching by the diabatically heated updraughts will increase the amplitude of the vorticity. Thus the tilting mechanism provides a significant source of vertical vorticity for the storm development.

(d) Vertically-sheared ambient flow: strong shear

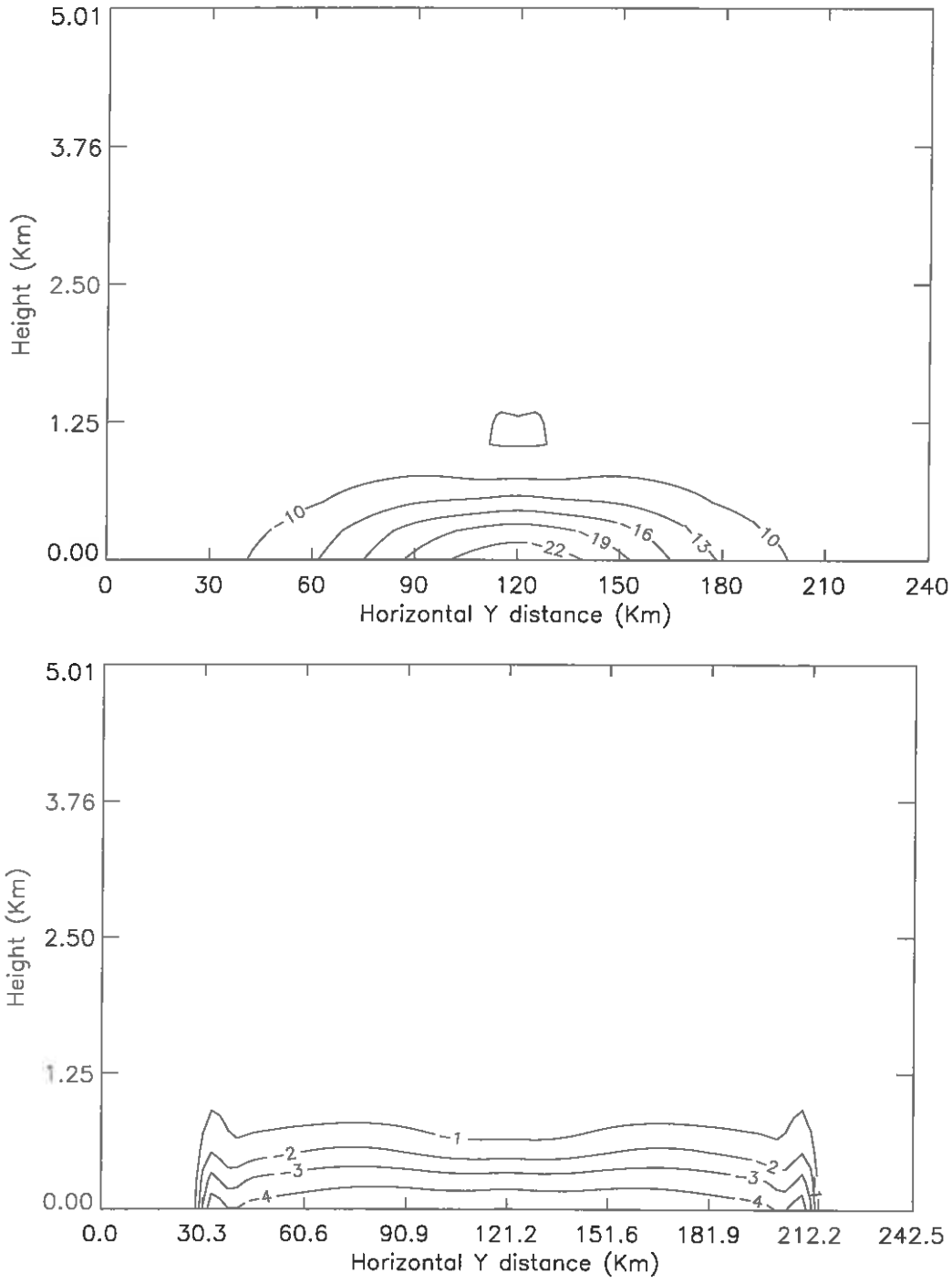

Figure 5: A y-z section across the broadest section of the cold pool showing the u-velocity (out of the plane; ms^{-1}) and the potential temperature (in K), for a uniform ambient flow of magnitude 10 ms^{-1} into the plane. Since the cold pool has spread downstream of the source, the diabtically cooled region does not appear in this figure.

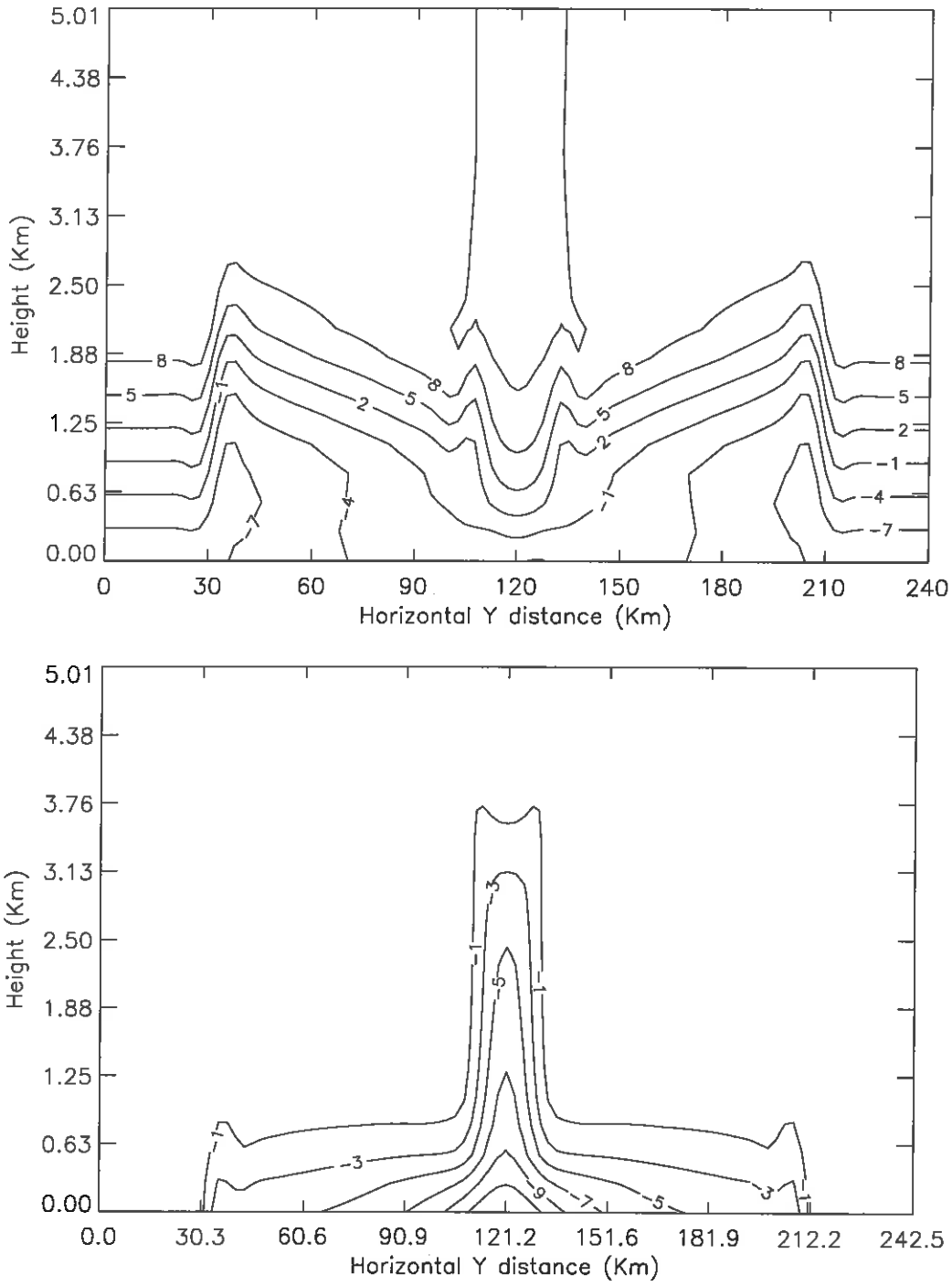

Figure 6: A y-z section across the cold pool (perpendicular to the ambient shear vector), showing the u-velocity (out of the plane; $/ms^{-1}$) and the potential temperature $(/K)$, for the sheared ambient flow of figure 1(d).

The cold pools modelled here emanate from a source which takes the form of a column of fixed cooling. When extremely intense (rather unphysical) ambient shear of $30ms^{-1}km^{-1}$, with ground level wind $-30ms^{-1}$, is imposed on this system, the column of cooled air is itself strongly deformed by the shear, being advected to the right aloft by the $60ms^{-1}$ wind and advected to the left at the ground, to produce elongation in the x-direction, and the effective source region at the ground is no longer circular. This effect can be seen in figure 1(f); a vertical cross-section through this flow illustrates how the elevated cold air becomes extended in the x-direction. As such, this deforming of the gravity current is not in this case seen as an interaction between the spreading cold air and the ambient shear, but rather as an interaction between the elevated source region and the shear. The results of Droegemeier and Wilhelmson (1985b) which show elongation of a storm-generated cold pool in ambient shear may stem from this process.

When this extremely strong shear is set to zero above a height of 1 km, with the same ground level wind, the severe distortion of the cold air aloft does not occur and a near-circular form evolves, comparable with that seen in figure 1(d).

Discussion and Conclusions

It has been found, by performing extremely simplified numerical simulations of gravity currents in sheared ambient flows, scaled to represent the cold pools of cumulonimbus systems, that the gravity currents are robust to the environmental shear in this regime. The plan form of the gravity current from an isolated source is not qualitatively influenced by the shear. Within the physically relevant regime of ambient winds for the study of such storm-generated cold pools, it seems that the shape of the spreading region of cold air can be dependent more on the ambient wind strength than the ambient shear. As a consequence, the modelled behaviour of intense storms, in which near-circular vortices form and may cause significant storm development such as updraught splitting, is likely to be due to the intense vortex stretching and tilting induced by the convection. It must be recalled, however, that a principal effect of shear on a gravity current is to deepen its downshear edge, creating more favourable conditions for triggering of convection. This model illustrates the way in which the tilting of ambient vortex tubes generates regions of high vertical vorticity which may be intensified and organised by the moist convection and which are of opposite sign to that which occurs in the absence of environmental shear. The extension of these ideas to general cases would require more extensive study over a wider parameter regime.

In this system, with a free-slip boundary condition at the ground, the reference frame is determined by the reference frame of the cooling region. The amplitude of the ambient wind is determined relative to the region of cooling. It has been shown how a strong ambient wind may change the characteristics of the spreading cold pool, by bringing the leading edge to stagnation relative to the source, while the gravity current continues to spread in other directions. This phenomenon relates to an apparent discrepancy between numerical simulations of convective storm cold pools and laboratory gravity currents (such as those of Linden and Simpson, 1994) in which the upstream head is shallower than the downstream one; this discrepancy is likely to be due to the jet-like or plume-like nature of the source. Furthermore, the interaction of the source with the ambient shear generates a rear-inflow jet and, in extremely strong shear, causes a deforming of the source air at the ground, along the direction of the shear (figure 1(f)). From these observations, it seems that the interaction between the source of cooling and the ambient wind is a stronger one than that between the 'free' gravity current and the shear. Effectively,

this is to conclude that the cloud processes above a cold pool have a stronger bearing on the development of the system than the cold pool dynamics. In this model the cooling region is artificially simple and does not attempt to simulate cloud dynamics.

The numerical simulations discussed here have been designed to be as simple as possible, to illuminate the essentials of the dynamics. Processes which may have a bearing on the validity of these results include planetary rotation, the influence of static stability, rotation of the shear vector with height and effects of turbulence and surface drag. In addition, it must always be accepted that a numerical model such as this may exhibit instabilities and dynamics of its own. Since numerical simulations of cumulonimbus convection are now widespread, an understanding of the processes within these models is desirable, though links with physical flows must always be maintained. The essential consistency of the results, from the simple cases in a quiescent environment, which seem to agree with analytic and experimental work, to the cold pools in more complex ambient flows, suggests that the qualitative picture given here is correct. Further confirmation of this is only likely to be obtained by very sophisticated laboratory or numerical modelling.

Acknowledgements.

I wish to thank Alan Thorpe for his help and advice on this problem. I have also enjoyed interesting discussions with Rich Rotunno, Morris Weisman, Bill Skamarock and others. During the progress of this reseach I have been supported by an NERC grant.

References

Benjamin, T.B., 1968, 'Gravity currents and related phenomena', J. Fluid Mech., **31**, 209-248.

Britter R.E., 1979, 'The spread of a negatively buoyant plume in a calm environment', Atmos. Environ., **13**, 1241-1247.

Davis C.A. and Weisman, M.L., 1994, 'Balanced dynamics of mesoscale vortices produced in simulated convective systems', J. Atmos. Sci., **51**, 2005-2030.

Droegemeier K.K. and Wilhelmson, R.B., 1985a, 'Three-dimensional numerical modelling of convection produced by interacting thunderstorm outflows. Part I: Control simulation and low level moisture variations', J. Atmos. Sci., **42**, 2381-2403.

Droegemeier K.K. and Wilhelmson, R.B., 1985b, 'Three-dimensional numericalmodelling of convection produced by interacting thunderstorm outflows. Part II: Variations in vertical wind shear', J. Atmos. Sci., **42**, 2404-2414.

Klemp, J.B., Rotunno, R. and Skamarock, W.C., 1991, 'On the dynamics of gravity currents in a channel', J. Fluid Mech., **269**, 169-198.

Linden, P.F. and Simpson, J.E., 1994, 'Continuous releases of dense fluid from an elevated point source in a cross-flow', *Mixing and Transport in the Environment*, Ed. K.J. Beven, P.C. Chatwin and J.H. Millbank, Wiley.

Meischner, P.F., Bringi, V.N., Heimann, D. and Holler, H., 1991, 'A squall line in southern Germany: kinematics and precipitation formation as deduced by advanced polarimetric and Doppler radar measurements', Mon. Wea. Rev., **115**, 678-701.

Miranda, P.M.A., 1990, 'Gravity waves and wave drag in flow past three-dimensional isolated mountains', PhD Thesis, University of Reading, 190pp.

Rotunno, R., Klemp, J.B. and Weisman, M.L., 1988, 'A theory for strong, long-lived squall lines', J. Atmos. Sci., **45**, 463-485.

Raymond, D.J. and Rotunno, R., 1989 'Response of a stably stratified flow to cooling', J. Atmos. Sci., **46**, 2830-2837.

Simpson, J.E., 1982, 'Gravity currents in the laboratory, atmosphere and ocean', Ann. Rev. Fluid Mech., **14**, 213-234.

Simpson, J.E. and Britter R.E., 1980, 'A laboratory model of an atmospheric mesofront', Q. J. R. Meteorol. Soc., **106**, 485-500.

Smith, R.K. and Reeder, M.J., 1988, 'On the movement and low-level structure of cold fronts', Mon. Wea. Rev., **116**, 1927-1944.

Thorpe, A.J., Miller, M.J. and Moncrieff, M.W., 1980, 'Dynamical models of two-dimensional downdraughts', Q. J. R. Meteorol. Soc., **106**, 463-484.

Thorpe, A.J., Miller, M.J. and Moncrieff, M.W., 1982, 'Two-dimensional convection in non-constant shear: a model of mid-latitude squall lines', Q. J. R. Meteorol. Soc., **108**, 739-762.

Weisman, M.L., 1993, 'The genesis of severe, long-lived bow-echoes', J. Atmos. Sci., **50**, 645-670.

Xu, Q., 1992, 'Density currents in shear flows-a two-fluid model', J. Atmos. Sci., **49**, 511-524.

CURRENT JCMM INTERNAL REPORTS

This series of JCMM Internal Reports, initiated in 1993, contains unpublished reports and also versions of articles submitted for publication. The complete set of Internal Reports is available from the National Meteorology Library on loan, if required.

1. **Research Strategy and Programme.**
   K A Browning et al
   January 1993

2. **The GEWEX Cloud System Study (GCSS).**
   GEWEX Cloud System Science Team
   January 1993

3. **Evolution of a mesoscale upper tropospheric vorticity maximum and comma cloud from a cloud-free two-dimensional potential vorticity anomaly.**
   K A Browning
   January 1993

4. **The Global Energy and Water Cycle**
   K A Browning
   July 1993

5. **Structure of a midlatitude cyclone before occlusion.**
   K A Browning and N Roberts
   July 1993

6. **Developments in Systems and Tools for Weather Forecasting.**
   K A Browning and G Szejwach
   July 1993

7. **Diagnostic study of a narrow cold frontal rainband and severe winds associated with a stratospheric intrusion.**
   K A Browning and R Reynolds
   August 1993

8. **Survey of perceived priority issues in the parametrizations of cloud-related processes in GCMs.**
   K A Browning
   September 1993

9. **The Effect of Rain on Longwave Radiation.**
   I Dharssi
   September 1993

10. **Cloud Microphysical Processes - A Description of the Parametrization used in the Large Eddy Model.**
H Swann
July 1994

11. **An Appreciation of the Meteorological Research of Ernst Kleinschmidt.**
A J Thorpe
May 1992

12. **Potential Vorticity of Flow Along the Alps.**
A J Thorpe, H Volkert and Dietrich Heimann
August 1992

13. **The Representation of Fronts.**
A J Thorpe
January 1993

14. **A Parametrization Scheme for Symmetric Instability: Tests for an Idealised Flow.**
C S Chan and A J Thorpe
February 1993

15. **The Fronts 92 Experiment: a Quicklook Atlas.**
Edited by T D Hewson
November 1993

16. **Frontal wave stability during moist deformation frontogenesis. Part 1. Linear wave dynamics**
C H Bishop and A J Thorpe
May 1993

17. **Frontal wave stability during moist deformation frontogenesis. Part 2. The suppression of non-linear wave development.**
C H Bishop and A J Thorpe
May 1993

18. **Gravity waves in sheared ducts.**
S Monserrat and A J Thorpe
October 1993

19. **Potential Vorticity and the Electrostatics Analogy: Quasi-Geostrophic Theory.**
C Bishop and A J Thorpe
November 1993

20. **Recent Advances in the Measurement of Precipitation by Radar.**
A J Illingworth
April 1993

21. **Micro-Physique et Givrage. Cloud Microphysics and Aircraft Icing.**
A J Illingworth
May 1993

22. **Differential Phase Measurements of Precipitation.**
M Blackman and A J Illingworth
May 1993

23. **Estimation of Effective Radius of Cloud Particles from the Radar Reflectivity.**
N I Fox and A J Illingworth
May 1993

24. **A Simple Method of Dopplerising a Pulsed Magnetron Radar.**
L Hua, A J Illingworth and J Eastment
November 1993

25. **Radiation and Polar Lows.**
George C Craig
February 1994

26. **Collected preprints submitted to International Symposium on the Life Cycles of Extratropical Cyclones; Bergen, Norway, 27 June - 1 July 1994**
April 1994

27. **Convective Frontogenesis**
Douglas J Parker and Alan J Thorpe
April 1994

28. **Improved Measurement Of The Ice Water Content In Cirrus Using A Total Water Evaporator**
Philip R A Brown and Peter N Francis
April 1994

29. **Mesoscale Effects of a Dry Intrusion within a Vigorous Cyclone**
K A Browning and B W Golding
April 1994

30. **GEWEX Cloud System Study, Science Plan**
May 1994

31. **Parametrization of Momentum Transport by Convectively Generated Gravity Waves**
R Kershaw
February 1995

32. **Mesoscale Modelling Newsletter, No. 5**
May 1994

33. **Observations of the mesoscale sub-structure in the cold air of a developing frontal cyclone**
K A Browning, S A Clough, C S A Davitt, N M Roberts and T D Hewson
May 1994

34. **Longwave Radiative Forcing of a Simulated Tropical Squall Line**
Imtiaz Dharssi
July 1994

35. **On the nature of the convective circulations at a kata-cold front**
K A Browning
September 1994

36. **Collected preprints of papers submitted to the COST-75 International Seminar on Advanced Weather Radar Systems, Brussels, 20-23 September 1994**
November 1994

37. **Use of satellite imagery to diagnose events leading to frontal thunderstorms: Parts I and II of a case study**
K A Browning and N M Roberts
November 1994

38. **The role of spaceborne millimetre-wave radar in the global monitoring of ice cloud**
P R A Brown, A J Illingworth, A J Heymsfield, G M McFarquhar, K A Browning and M Gosset
December 1994

39. **Potential Vorticity Inversion**
Michal Ziemianski
October 1994

40. **Theory of mature tropical cyclones; A comparison between Kleinschmidt (1951) and Emanual (1986)**
Suzanne L Gray
December 1994

41. **Dispersion and removal of pollutants during the passage of an atmospheric frontal system**
N R Gimson
December 1994

42. **The role of snow sublimation in frontogenesis**
D J Parker and A J Thorpe
December 1994

43. **Potential vorticity and the electrostatics Analogy: Ertel-Rossby formulation**
A J Thorpe and C H Bishop
December 1994

44. **Mesoscale aspects of extratropical cyclones: an observational perspective**
K A Browning
January 1995

45. **A Polar Low Outbreak: Evolution and Mesoscale Structures**
T D Hewson, G C Craig and C Claud
February 1995

46. **Generation of near-surface gusts by deep convection**
K Nakamura and R Kershaw
April 1995

47. **Attribution concepts applied to the omega equation**
S A Clough, C S A Davitt and A J Thorpe
June 1995

48 **Parametrization of mixed-phase cloud and precipitation**
Susan P Ballard and M Gerard Hutchinson
June 1995

49 **Short-range forecasting of stratocumulus: Initialization V Prediction**
Susan P Ballard, Simon D Jackson and B Macpherson
June 1995

50 **Contributions of the JCMM/Dept of Meteorology Radar Group to the 27th AMS Radar Meteorology Conference, Vail October 1995**
June 1995

51 **Cold pools in shear**
Douglas J Parker
September 1995

Met Office Joint Centre for Mesoscale Meteorology Department of Meteorology
University of Reading PO Box 243 Reading RG6 6BB United Kingdom
Tel: +44 (0)118 931 8425 Fax: +44 (0)118 931 8791
www.metoffice.com